Journal of Physics: Conference Series **109** (2008) 012002 doi:10.1088/1742-6596/109/1/012002

Electrical properties of carbon nanotube FETs

T Mizutani, Y Nosho and Y Ohno
Department of Quantum Engineering, Nagoya University, Furo-cho, Chikusa-ku, Nagoya 464-8603, Japan

E-mail:tmizu@nuee.nagoya-u.ac.jp

The electrical properties of carbon nanotube FETs (CNTFETs) have been studied in detail. The conduction type of the CNTFETs was dependent on the work function of the contact metal, which suggests that Fermi level pinning at the metal/nanotube interface does not happen. Based on the two-probe and four-probe resistance measurements, it was shown that the carrier transport at the contact is explained by the edge contact model even in the diffusive regime. The chemical doping using F_4TCNQ was effective to reduce not only the channel resistance but also the contact resistance.
It has also been shown that the surface potential measurement based on the electrostatic force detection in the scanning probe microscopy was effective in studying the behavior of the CNTFETs such as the transient behavior and the effect of the defects. Finally, in the CNTFETs fabricated using plasma-enhanced (PE) CVD-grown nanotubes, most of the drain current could be modulated by the gate voltage with little non-depletable drain current suggesting the preferential growth of the nanotubes with semiconducting behavior.

1. Introduction

Carbon nanotube FETs (CNTFETs) are expected to offer high-performance electronic and optoelectronic devices because they have advantages such as a high electron velocity, a high current driving capability and an energy band structure with direct transition [1, 2]. However, understandings of the device operation are not sufficient. In this paper, electrical characteristics of the CNTFETs such as the dependence of the conduction type of the CNTFETs on the work function of the contact metal, current transport at the contact, effects of the chemical doping, and preferential growth of the CNTs with semiconducting behavior in the CNTFET channel will be reported.

2. Electrical properties of the CNT-FETs

2.1. Dependence on the work function of the contact metal

The operation of the device with back gate (BG) is explained by the Schottky barrier transistor model [3, 4] where the Schottky barrier formed at the contact which determines the carrier injection from the contacts is controlled by the gate voltage. In such model, we can expect *I-V* characteristics are dependent on the work function of the contact metal because Schottky barrier height is dependent on the work function.

In order to study the effects of the work function of the contact metal, we have fabricated CNTFETs using various contact metals with different work functions on the heavily-doped Si substrate. Figure 1 is the drain current as a function of the gate voltage for various contact metals [5]. The conduction type was dependent on the work function as shown in the figure. In the case of the Pd with a large work function (5.1 eV), drain current increases with decrease in the gate voltage, indicating the p-type conduction. In the case of Ca with a small work function (2.9 eV), n-type conduction was observed on the other hand and ambipolar behavior for the Mg with a work function of the medium value (3.7 eV).

These results can be understood if we take into account the band diagram shown in the insets of Fig. 1 and are consistent with the Schottky barrier transistor model. That is, as schematically illustrated in the insets, the Fermi level (E_F) of the source electrodes would be positioned close to the valence band (E_V) for the contact metal with a large work function. In this case, the holes are easily injected into the nanotube. The ambipolar characteristics observed in the Mg-CNTFET suggest that the E_F is positioned at around the middle of the band gap of the nanotube. In this case, it is possible to inject both electrons and holes into the nanotube depending on the polarity of V_{GS}. In the case of the Ca-CNTFET in which the *n*-type conduction property is realized, the E_F of the Ca contact is thought to be positioned close to the conduction band (E_C) of the nanotube. The work function dependent behavior suggests that Fermi level pinning at the metal/nanotube interface does not happen in the CNTs.

2.2. Quasi pn diodes

If we take advantage of the work function dependence of the *I-V* characteristics, it is possible to implement quasi pn diode using different contact metals for anode and cathode without any impurity doping. Figure 2 shows *I-V* characteristics of the quasi pn diode in which Pd and Ca are used for the anode and cathode, respectively. Rectifying behavior is obtained in the quasi pn diode as shown in the figure. The insets show schematic band diagrams of the nanotube diode at forward and reverse biases, respectively, which explains the rectifying behavior.

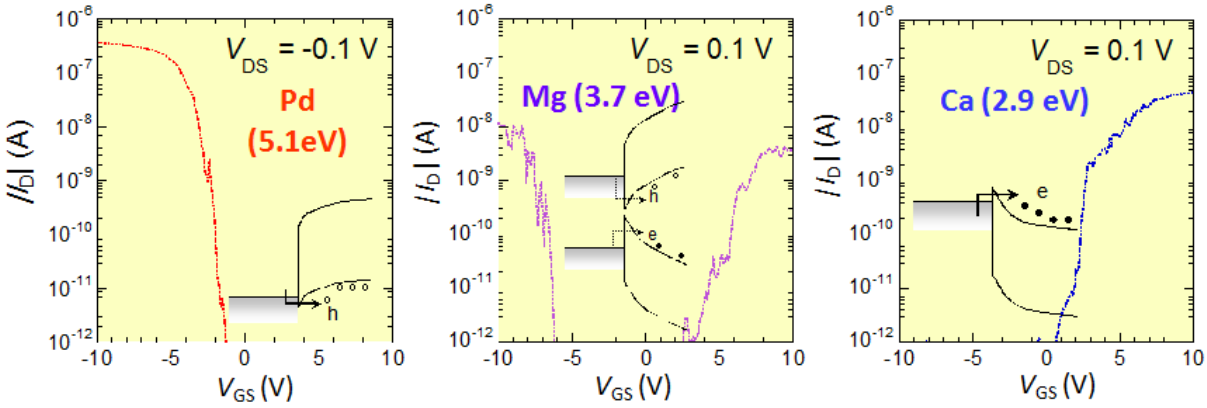

Figure 1. Drain current as a function of the gate voltage for various contact metals.

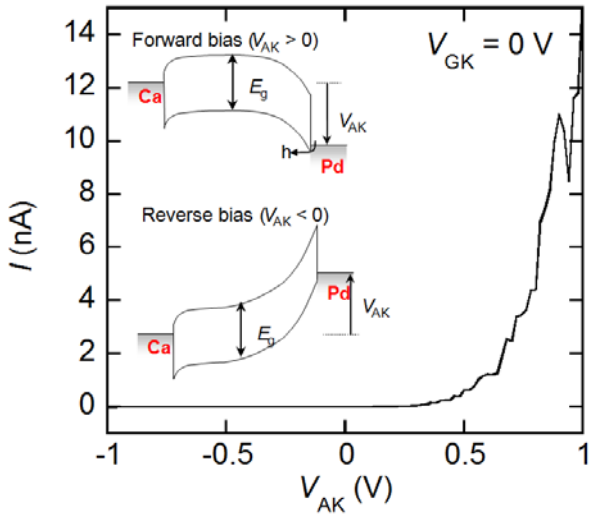

Figure 2. *I-V* characteristics of the nanotube quasi-*pn* diode. The insets show schematic band diagrams of the nanotube diode at forward and reverse biases, respectively.

2.3. Contact resistance

The Schottky barrier formed at the metal/nanotube interface will dominate the contact resistance (R_C). In order to evaluate R_C and channel resistance (R_{ch}) multi-terminal devices have been fabricated, as shown in Fig. 3 [6]. Figure 4(a) shows measured two-probe ($R2$, solid circles) and four-probe ($R4$, solid triangles) resistances of the device as a function of the channel length. The two-probe resistance and the four-probe resistance is almost same as shown in the figure. This result is contrary to expectation. In the case of standard semiconductors, the two-probe resistance is larger than the four-probe resistance because the contact resistance should be excluded in the case of four-probe resistance. The result of almost same values for $R2$ and $R4$ indicates that the contact resistance is included even in the four-probe measurement. This is possible if the equivalent circuit is expressed not by that in Fig. 4(b) but by that in Fig. 4(c) where the current does not pass through the CNT underneath the electrode and is picked up at the contact edge. This means that the current through the CNT channel is explained by the edge contact model even in the diffusive regime. The conductivity of the nanotube under the contact electrodes seems to be degraded.

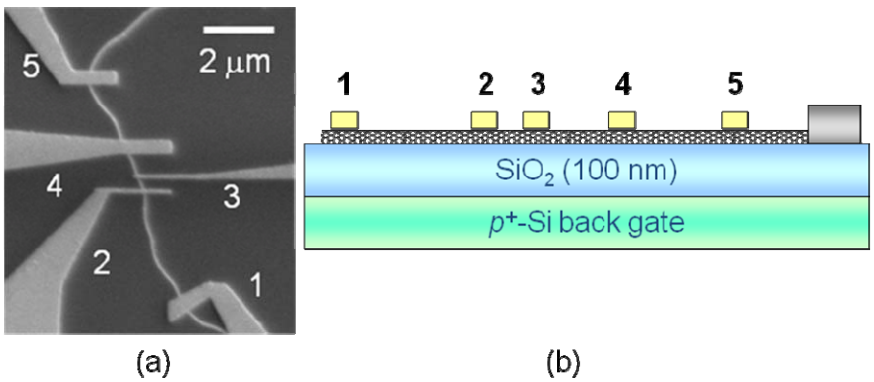

Figure 3. (a) SEM image and (b) schematic device structure of multi-terminal BG-CNTFET.

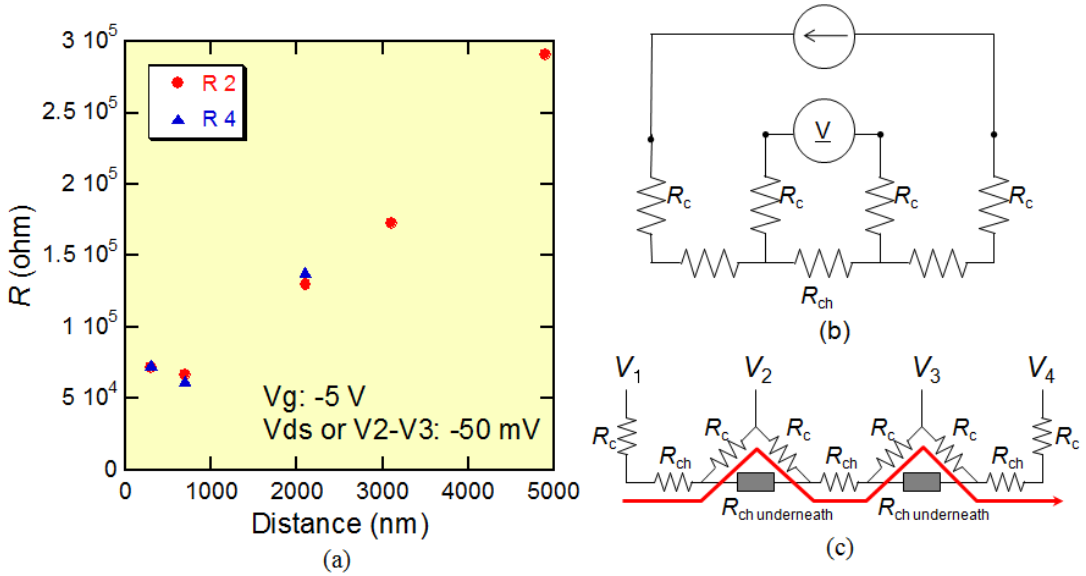

Figure 4. (a) Two-probe and four-probe resistances of the device as a function of the channel length. (b) and (c) are the equivalent circuits explaining the principle of the four-probe resistance and the edge contact model, respectively.

2.4. Chemical p-type doping

In order to decrease the parasitic source resistance in the CNTFETs, chemical p-type doping was performed using F_4TCNQ with a large electron affinity [7]. Following the electrode formation for the source/drain and the gate, the devices were soaked in the F_4TCNQ solution for 30 min for the chemical doping. Then, the self-aligned doping to the electrodes was realized. Figure 5 shows transmission-line-model plots of a multi-terminal BG-CNTFET before (dot) and after (triangle) F_4TCNQ chemical doping. The result shows that not only the R_{ch} but also the R_C were reduced by the F_4TCNQ doping. This result clearly shows that the chemical doping in the CNTFETs affects not only the Fermi level in the nanotube channel but also the energy-level alignment in the vicinity of the contacts leading to the reduction of the R_C. F_4TCNQ with a large electron affinity adsorbed at the vicinity of the contact edge is expected to form an interface dipole causing an abrupt potential change in the nanotube as shown in Fig. 6. This results in a lowering of the effective Schottky barrier height and consequent increase in the tunnelling probability of holes. Even though the F_4TCNQ molecules would not penetrate into the interface between the nanotube and the Au electrode deposited on the nanotube, it is reasonable to consider that the F_4TCNQ chemical doping affects the carrier transport at the contacts if we take into account the fact that carrier injection from the contact electrode into the nanotube occurs only at the edge of the electrodes. Even though the R_C dominates the source resistance before the doping, R_{ch} dominates the source resistance after doping due to a larger reduction of the R_C than that of the R_{ch}.

The chemical p-doping technique was applied to the top-gate CNTFETs. One order larger drain current and one order larger transconductance have been realized by the p-doping, as shown in Fig. 7. The maximum transconductance was 5 S/mm for the gate length of 0.2 μm. This is several times larger than that of the state-of-the-art Si MOSFET technology.

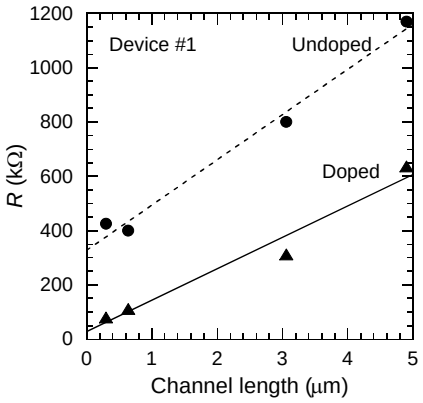

Figure 5. Two-probe resistance before and after F_4TCNQ chemical doping as a function of the channel length at V_{DS} = -10 mV and V_{BG} = -5 V.

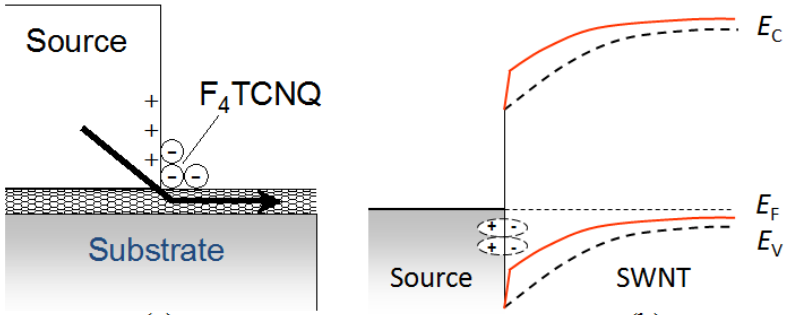

Figure 6. (a) Carrier flow path at the source contact. Holes are injected into the nanotube at the edge of the contact electrode. (b) Schematic energy band structure before doping (dashed line) and after doping (solid line) at no bias condition. F_4TCNQ molecules adsorbed at the vicinity of the contact form the dipoles between the source and nanotube, resulting in abrupt potential change at the interface.

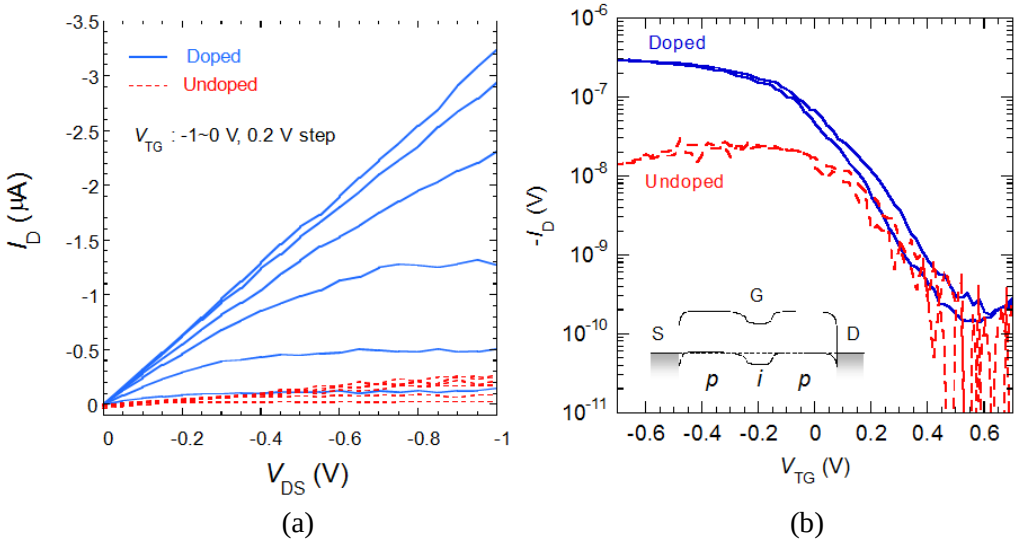

Figure 7. Chemical doping using F_4TCNQ. (a) I_D-V_{DS} and (b) I_D-V_{TG} characteristics of the top-gate CNTFET. Dotted and solid lines are the results of the device before and after chemical doping.

2.5. Preferential growth of nanotubes with semiconducting behavior

One of the most important issues which should be addressed for implementing CNTFET integrated circuits is the preferential growth of the semiconducting nanotubes, because metallic nanotubes result in poor current-voltage characteristics with nondepletable current (small ON/OFF ratio), resulting in a excess power dissipation. Figure 8 shows the statistics of the drain current for many CNTFETs in which many nanotube channels were bridging between source and drain electrodes [8]. Here, the nanotubes were grown by grid-inserted PECVD to suppress the ion bombardment damage [9]. Depletable and nondepletable currents shown by dark and bright bars correspond to the semiconducting and metallic/quasi-metallic nanotubes, respectively. The component of the depletable current was more than 96 % of the total drain current. This indicates that the nanotubes with semiconducting behavior were preferentially grown by the present PECVD. Even though the mechanism of the preferential growth is not clear at present, plausible origin is chirality change during the growth or potential barrier formation by the defects in the CNT channel introduced during the growth. This is a subject for the future study.

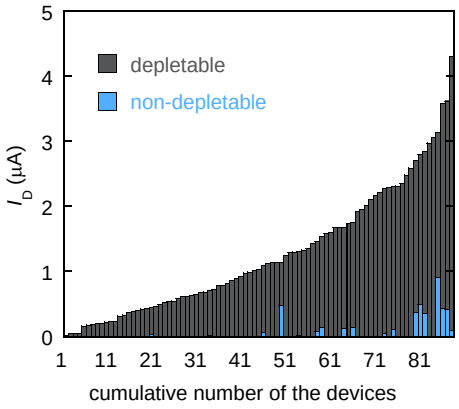

Figure 8. Depletable (dark bars) and nondepletable (bright bars) drain currents for many CNTFETs. V_{DS} = -1 V and V_{GS} = -10 V, respectively. The component of depletable current corresponding to the semiconducting nanotubes is very high (96 %).

2.6. Surface potential measurement

In order to fully understand the CNTFET operation, the surface potential of the CNTFETs was measured based on the electrostatic force detection in the scanning probe microscopy. Figure 9(a) and (b) are the surface potential image at the same bias voltage for different gate bias sequences measured in air atmosphere [10]. It is notable that the potential in the area around the CNT indicated by arrows differ from each other even though the gate bias voltages are the same (0 V). That is, the potential image is dependent on the gate bias sequence; (a) from -5 V to 0 V and (b) from +5 V to 0 V. This is consistent with the hysteresis of the current-voltage characteristic of the CNTFETs, where the drain current is dependent on the gate bias sequence. It seems that the mobile ions in the water molecules are responsible for the transient behaviors of the drain current and surface potential.

Figure 10(a) shows the AFM image, and (b) and (c) show the potential images measured in vacuum at gate bias voltages (V_{GS}) of -1 V (ON state) and 2 V (OFF state), respectively [11]. Even though the AFM image seems to be smooth with little feature, the potential image at the OFF state (V_{GS} = 2 V) shown in Fig. 10(c) shows non-uniform image with dark area (indicated by arrows). This indicates that the CNT channel was divided into multiple segments separated by the potential barriers which probably result from the effects of the defects in the CNT channel. It is notable that the potential image was smooth when the CNTFET was biased at ON state (V_{GS} = -1 V). Plausible origin why the potential was smooth at the ON state is screening of the trapped charge at the defects by the holes in

the CNT channel. Another possibility is the so-called conduction band flattening by the gate voltage at high hole concentration. Further study is required to clarify this point.

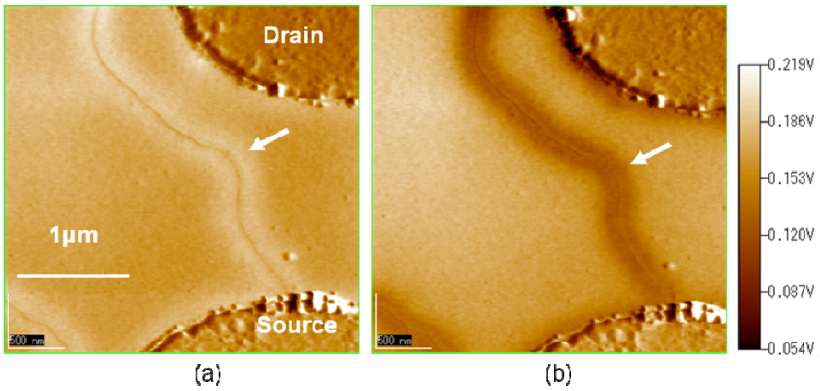

Figure 9. Surface potential images of the CNTFET at V_{GS} = 0 V and V_{DS} = -0.3 V measured in air atmosphere. (a) just after -5 V gate bias stress and (b) just after +5 V gate bias stress.

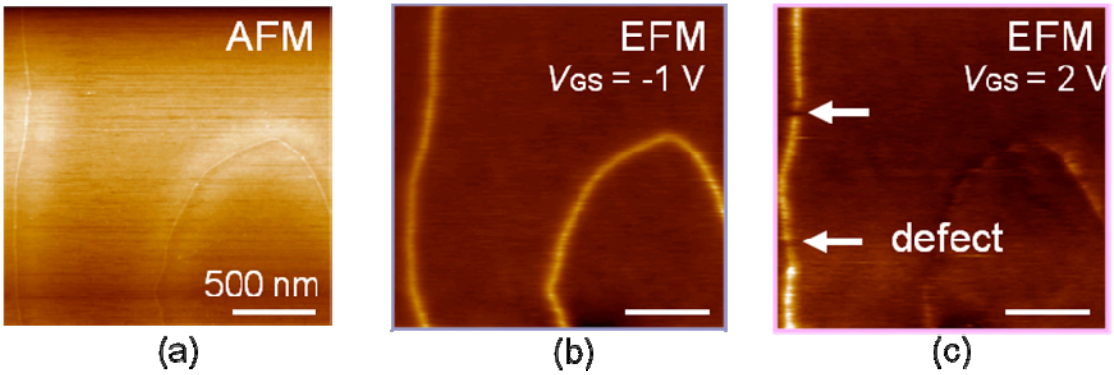

Figure 10. (a) Topographic image, (b) surface potential image at the ON state (V_{GS} = -1 V), and (c) surface potential image at the OFF state (V_{GS} = 2 V) measured in vacuum. The drain voltage (V_{DS}) was 0.3 V.

3. Summary

We have studied the effects of the work function of the contact metal on the current-voltage characteristics of the CNTFETs. The conduction type of the device was dependent on the work function of the contact metal. This suggests that the Fermi level pinning at the metal/nanotube interface does not happen. We have also shown that the chemical p-type doping using F_4TCNQ with a large electron affinity was effective to reduce not only the channel resistance but also the contact resistance. The reduction in the contact resistance of 1/10 was more prominent than that of the channel resistance. Top-gate CNTFETs fabricated by the self-aligned chemical doping at the access regions showed one-order larger transconductance.

It has also been shown that the carrier transport at the contact is explained by the edge contact model even in the diffusive regime based on the two-probe and four-probe resistance measurements. The surface potential measured by the detection of the electrostatic force between the cantilever tip and the device surface in air was dependent on the sequence of the gate bias. This is consistent with the drain current transient and hysteresis of the current-voltage characteristics of the CNTFETs. The surface potential measured in vacuum showed non-uniform potential profile which was probably due to the effect of the defects in the CNT channel.

In the CNTFETs with many nanotube channels bridging between source and drain electrodes fabricated using PECVD-grown nanotubes, most of the drain current could be modulated by the gate voltage with little non-depletable drain current. This suggests that the nanotubes with semiconducting behavior are preferentially grown by the PECVD.

Acknowledgements
This work was partially supported by the Grant-in-Aid for Scientific Research on Priority Area of MEXT.

References

[1] Rosenblattet S et al. 2005 Appl. Phys. Lett. **87** 153111
[2] Javey A, Guo J, Farmer D B, Wang Q, Yenilmez E, Gordon R G, Lundstrom M and Dai H 2004 Nano Lett.**7** 1319
[3] Heinze S, Tersoff J, Martel R, Derycke V, Appenzeller and Avouris Ph 2002 Phys. Rev. Lett. **89** 106801
[4] Mizutani T, Iwatsuki S, Ohno Y Kishimoto S 2005 Jpn. J. Appl. Phys. **44** 1599
[5] Nosho Y, Ohno Y, Kishimoto S and Mizutani T 2006 Nanotechnology **17** 3412
[6] Nosho Y, Ohno Y, Kishimoto S and Mizutani T 2007 Jpn. J. Appl. Phys. **46** L474
[7] Nosho Y, Ohno Y, Kishimoto S and Mizutani T 2007 Nanotechnology **18** 415202
[8] Ohnaka H, Kojima Y, Kishimoto S, Ohno Y and Mizutani T 2006 Jpn. J. Appl. Phys. **45** 5485
[9] Kojima Y, Kishimoto s, Ohno Y, Sakai A and Mizutani T 2005 Jpn. J. Appl. Phys. **44** 2600
[10] Umesaka T, Ohnaka H, Ohno Y, Kishimoto S, K. Maezawa and Mizutani T 2007 Jpn. J. Appl. Phys. **46** 2496
[11] Okigawa Y, Umesaka T, Ohno Y, Kishimoto S and Mizutani T 2007 Int. Symp. Compound Semiconductors Kyoto Japan TuC II-4